

Ocean currents shape the genetic structure of the kelp *Laminaria pallida* in southwestern Africa

Jorge Assis^{1*}, João Neiva^{1*}, John J. Bolton², Mark D. Rothman^{2,3}, Licínia Gouveia¹, Cristina Paulino¹, Hasliza Mohdnasir¹, Robert J. Anderson², Maggie M. Reddy², Lineekela Kandjengo⁴, Anja Kreiner⁵, Gareth A. Pearson^{1**}, Ester A. Serrão^{1**}

¹CCMAR, University of Algarve, Gambelas, Faro, Portugal

²Department of Biological Sciences, University of Cape Town, South Africa

³Department of Forestry, Fisheries and the Environment, Cape Town, South Africa

⁴University of Namibia, Sam Nujoma Marine and Coastal Resources Research Centre, Henties Bay, Namibia

⁵National Marine Information and Research Centre, Ministry of Fisheries and Marine Resources, Swakopmund, Namibia

Corresponding author: Jorge Assis (jorgemfa@gmail.com; +351 912361127) and Ester Serrão (eserrao@ualg.pt; +351 965375631)

* and ** authors contributed equally to this work

24 **Abstract**

25 Aim: Drivers of extant population genetic structure include past climate-driven range shifts
26 and vicariant events, as well as gene flow mediated by dispersal and habitat continuity. Their
27 integration as alternative or complementary drivers is however often missing or incomplete,
28 potentially overlooking relevant processes and time scales. Here we ask whether it is the
29 imprint of past range shifts or habitat connectivity driven by oceanographic transport that
30 best explain genetic structure in a poorly understood model, a forest-forming African kelp.

31 Location: Southwestern coast of Africa (Benguela current region).

32 Taxon: *Laminaria pallida*.

33 Methods: We estimated genetic variability along the species distributional range using 14
34 microsatellite markers. This was compared to estimates of past range shifts derived from
35 species distribution modelling for the Last Glacial Maximum (LGM), the mid-Holocene (MH)
36 and the present, and estimates of habitat connectivity derived from oceanographic
37 biophysical modelling.

38 Results: The species is structured in two well-defined clusters, a southern cluster with much
39 richer (allelic richness $A: 10.40 \pm 0.33$) and unique (private alleles $PA: 56.69 \pm 4.05$) genetic
40 diversity, and a northern cluster ($A: 4.75 \pm 0.17$; $PA: 6.70 \pm 1.45$). These clusters matched well-
41 known biogeographic regions and their transition coincided with a dispersal barrier formed
42 by upwelled offshore transport. No major climate-driven range shifts or vicariant events were
43 hindcasted along the present range, suggesting population stability from the LGM to the
44 present.

45 Main conclusions: Habitat connectivity, rather than past range shifts, explains the extant
46 population structure. Future environmental requirements of the species along the Benguela
47 upwelling system are projected to persist or even intensify, likely preserving the observed

genetic patterns for the years to come. Yet, the differentiation and endemism between genetic groups, and the inferred isolation structured by the regional oceanography, implies high conservation value for genetic biodiversity, and even more if considering the multiple ecological, social, and economic services provided by kelp forests.

68 **Introduction**

69 Marine species exhibit considerable variation in their dispersal potential, ranging from near
70 panmixia to highly structured meta-populations. Sessile organisms lacking long-lived
71 dispersive stages (e.g., pelagic larvae) tend to exhibit relatively short dispersal kernels and
72 considerable population genetic structure across their ranges. This often reflects the imprints
73 left from past events, such as vicariance and range shifts experienced throughout glacial-
74 interglacial cycles (Assis et al., 2016, 2018; Maggs et al., 2008; Phair et al., 2019; Song et al.,
75 2021; Toms et al., 2014). In particular, endemic lineages often coincide where species
76 persisted during both cold and warm climatic extremes (i.e., within climatic refugia), while
77 more recently colonized areas tend to show homogeneous populations with reduced
78 diversity owing to genetic bottlenecks resulting from founder effects. Dispersal can further
79 influence population genetic structure, maintaining or diluting the imprints of past events
80 (Alberto et al., 2011; Assis et al., 2018; Buonomo et al., 2016; Lourenço et al., 2017; Silva et
81 al., 2014). While main oceanographic processes (e.g., upwelling) can help preserve genetic
82 differentiation (Henriques et al., 2014, 2016), periodic events characterized by strong
83 oceanographic currents or upwelling disruptions can promote long distance connectivity and
84 gene flow, even for low dispersal species (Batista et al., 2018; Gunawickrama et al., 2020).
85 Disentangling the potential drivers of population genetic structure has much biogeographical
86 and evolutionary relevance (Assis et al., 2018), as well as conservation and management
87 implications (Mertens et al., 2018; Nepper-Davidsen et al., 2021), but their integration is often
88 neglected, potentially leading to conclusions biased towards the particular process analysed,
89 and overlooking their relative mutual influence.

90 Southwestern Africa is an ideal region to explore the potential drivers of population genetic
91 structure, owing to its linear coastline with sharp environmental gradients over short
92 geographic distances. The region is dominated by upwelling from the northward-flowing
93 Benguela current, which results in one of the world's most important eastern boundary

94 upwelling systems (Kämpf & Chapman, 2016). This sustains the very productive Benguela
95 province (Spalding et al., 2007), which includes major sub-Saharan kelp forest ecosystems
96 (Rothman, Bolton, et al., 2017). To the north, this region is delimited by the Angolan
97 ecoregion, where a sharp transition to tropical conditions and communities occurs (Anderson
98 et al., 2012; Spalding et al., 2007). Drivers of marine population structure along southwestern
99 Africa remain insufficiently documented, but high levels of intraspecific genetic variation have
100 been reported for several species of fish and invertebrates. Genetic breaks can vary
101 considerably (Teske et al., 2011; Von der Heyden et al., 2013), but some congruence has
102 been found, with species displaying distinct lineages (and even sibling species) within well-
103 defined regions (Evans et al., 2004; Henriques et al., 2014, 2016; Reid et al., 2016; Schulze
104 et al., 2020; Teske et al., 2006). Studies have attributed the observed patterns to life-history
105 traits and contemporary selection (Phair et al., 2019; Teske et al., 2019), paleoceanographic
106 sea-level changes (down to -120 m during the Last Glacial Maximum, LGM, ca. 20,000 years
107 ago) and associated coastline displacements (Toms et al., 2014), as well as oceanographic
108 transport and its inherent processes (Gunawickrama et al., 2020; Henriques et al., 2012,
109 2014, 2016; Schulze et al., 2020). In particular, the strong upwelling front centred off Lüderitz
110 (approx. 26°S latitude) promotes powerful offshore advection of Benguela current and
111 represents a permanent dispersal barrier for numerous marine species inhabiting the region
112 (Gunawickrama et al., 2020; Henriques et al., 2012, 2014, 2016; Schulze et al., 2020) and is
113 a general marine biogeographic break (Spalding et al. 2017). The impact of past climate-
114 driven range shifts has not been recognized as a major driver of genetic structure in
115 southwestern Africa (Nielsen et al., 2021), contrasting to what has been widely suggested in
116 the Northeast Atlantic and the Southwest and Northwest Pacific (Assis et al., 2016, 2018;
117 Fraser et al., 2009; Neiva et al., 2018; Song et al., 2021). Glacial advances could have not
118 impacted coastal distributions, as the southern continental limit of Africa lies at ca. 35°
119 latitude, well beyond the reach of glacial ice (Peltier, 2004). However, paleo species
120 distribution modelling (SDM) exploring climate-driven range shifts are limited in the region

(Robinson et al., 2017), and one of the few attempts there actually show the potential for past range shifts (Nielsen et al., 2021), likely related to the intensification of the Benguela upwelling system and/or the weakening of the warmer Agulhas current (Hutson, 1980; Romero et al., 2003; Thackeray, 2016).

Despite the efforts over the past decades, knowledge gaps persist for southwestern Africa. Phylogeographic research has been mostly performed with mtDNA markers, typically lacking resolution and prone to selection (Teske et al., 2018), remains heavily biased towards fish and invertebrate species with high dispersal potential, and largely overlooks the west coast Benguela upwelling region, despite its high levels of regional endemism (Teske et al., 2011).

The present study addresses some of these gaps, by asking whether genetic structure of the forest-forming African kelp *Laminaria pallida* is explained by past climate-driven range shifts and shoreline displacements associated with sea level changes, and/or habitat connectivity mediated by oceanographic transport. The species represents an ideal model to investigate the subject, owing to the limited spore dispersal of *Laminaria* species, which allows retention of the imprints of past changes, while local populations can saturate available rocky shore habitats and promote density barriers, further buffering the homogenizing effect of gene-flow. Additionally, long-range dispersal by rafting of *Laminaria* fronds or entangled in other floating seaweed is possible (Clarkin et al., 2012), extending dispersal distances and distributional ranges across biogeographic regions (Assis et al., 2018). These traits and processes have been reported for kelp elsewhere (Assis et al., 2016, 2018; Fraser et al., 2009; Neiva et al., 2018; Song et al., 2021), but never were never addressed in southwestern Africa, notwithstanding the regional economic and ecological importance of kelps, including the multiple ecosystem services provided (Blamey & Bolton, 2018).

We compared the species' genetic variability inferred from polymorphic microsatellite markers with estimates of past range shifts and habitat connectivity derived from distribution and biophysical modelling. We hypothesize that (1) climate changes associated with the

intensification of the Benguela upwelling system and the weakening of the Agulhas current (Hutson, 1980; Romero et al., 2003; Thackeray, 2016), coupled with coastline displacements associated with sea level changes (Toms et al., 2014), produced past range shifts and shaped the extant genetic structure of *Laminaria pallida*. In this process, (2) the classic paradigm of low latitude refugia (Assis et al., 2016, 2018; Maggs et al., 2008) is not hypothesized, since there is no evidence for the direct impact of glacial ice in the higher latitudes of southwestern Africa. Additionally, (3) connectivity between rocky habitats shaped by the major oceanographic patterns of the Benguela current, promoting asymmetrical long-distance dispersal (Stenevik et al., 2008) and semi-permanent upwelling conditions, are further hypothesized to have driven the genetic structure of the species. In particular, the upwelling front centered off Lüderitz should coincide with the genetic discontinuities of *L. pallida*, as inferred for numerous species there (Gunawickrama et al., 2020; Henriques et al., 2012, 2014, 2016; Schulze et al., 2020), while the fewer and patchier rocky reefs in the northern range (Fig. 1) played a role in structuring diversity patterns. We contribute to a broader understanding of the drivers of marine phylogeography along this unique region, particularly overlooked for species with limited dispersal. Moreover, describing the location and drivers of endemic genetic lineages of kelps is timely, as their global persistence is threatened by projected climate changes (Arafeh-Dalmau et al., 2020; Assis, Araújo, et al., 2017).

Methods

Study area and focal species

The study was performed along the full continental distributional range of *Laminaria pallida*, which covers the Benguela upwelling region, from ca. 100 km east of Cape Town to near the Kunene River in northern Namibia (Bolton & Stegenga, 2002). Some temperate islands where the species is reported to occur (Assis et al., 2020) were not included in the analyses. Due to its geographically variable morphology, the species was previously considered two species: the solid-stiped form *L. pallida* and the hollow-stiped form *L. schinzii* (Rothman, Bolton, et al., 2017; Rothman, Mattio, et al., 2017). However, these are now considered conspecific, with the solid-stiped form found at its southern subtidal distribution. Northward, the species becomes progressively abundant inshore, with its stipes becoming gradually hollower. The species represents a major rocky reef ecosystem in the Benguela upwelling region, dominating the lower intertidal and shallow depths (Rothman, Bolton, et al., 2017).

Genetic diversity and structure

Laminaria pallida populations were sampled from 20 sites between Rocky Point (Northern Namibia, -19.0° Lat.) and Stanford's Cove (Western Cape, South Africa, -34.5° Lat.; Table 1; Fig. 1). At each site, tissue samples were collected haphazardly in the low-intertidal zone by walking along the entire accessible population to collect up to 30 individuals, ensuring at least one meter between consecutive algae, or, when populations were very small and concentrated, that different individuals were collected. Six additional samples (sites 1-5; Table 1) were collected as drift material, primarily in northern Namibia, to investigate their putative origin and potential evidence for long-distance drift-mediated dispersal. Samples were individually stored and dehydrated in silica-gel crystals until DNA extraction.

Genomic DNA was extracted using the Nucleospin Multi-96 plant kit (Macherey-Nagel Duren, Germany), according to the manufacturer's protocol. Fourteen microsatellite loci were amplified to generate multi-locus genotypes in all individuals, following previously developed methods for congeneric species *L. ochroleuca* (Coelho et al., 2014) and *L. digitata* (Billot et al., 1998). Polymerase chain reactions (PCRs) were performed in 15 μ L total volume containing 1 \times GoTaq Flexi buffer, 1.5–2.0 mM MgCl₂, 125 μ M each dNTP, 0.2–0.5 μ M of labelled (FAM, NED, HEX, ROX) forward and 0.5 μ M simple reverse primers, 0.5–1 U GoTaq Flexi DNA Polymerase (Promega), and 1 μ L of 1:10 or 1:100 diluted DNA template. An initial denaturation step (94 °C, 5 min) was followed by 30 cycles of 94 °C for 30 s, a primer-specific annealing temperature (T_a) for 30 s and 72 °C for 45 s, ending with a final extension step at 72 °C for 10 min (see Table S1 for primer names, sequences, and a summary of amplification details). Amplified fragments were separated using an ABI PRISM capillary sequencer (Applied Biosystems, CCMAR, Portugal). Alleles were manually scored in STRand (Toonen & Hughes, 2001) independently by JN, LG and HM using the 500 LIZ™ size standard (Applied Biosystems). These data were tested for null alleles and neutrality with Microchecker (Van Oosterhout et al., 2004) and Popgene (Yeh & Boyle, 1997), respectively. See data availability section for multi-locus genotypes per site.

Genetic diversity was estimated as standardized allelic richness, Nei's gene diversity and number of private alleles using R software (R Development Core Team, 2021) with the package diversity (Keenan et al., 2013). The same statistics were computed for the most differentiated genetic clusters found (described in results below). Genetic structure was inferred with Structure (Pritchard et al., 2000) without any prior population assignments. A range of assumed clusters (K, from 1 to 10) was run 25 times using a burn-in of 1,000,000 iterations and a run-length of 1,000,000 iterations. The ΔK criterion (Evanno et al., 2005) inferred the likely number K clusters. Pairwise genetic differentiation between clusters was determined as Jost's D (Whitlock, 2011) with the R package diveRsity. Hierarchical analysis

of molecular variance (AMOVA) performed with Genodive (Meirmans & Van Tienderen, 2004) tested the clustering assignments of Structure. This was based on allele frequency information with 10,000 permutations, with variance components extracted between sites, within genetic clusters, and between genetic clusters.

Species distribution models to infer past range shifts

Range shifts from the LGM to the present were inferred with species distribution modelling using Boosted Regression Trees (BRT) and Adaptive Boosting (AdaBoost), two machine-learning algorithms known for high predictive performances and the ability to fit complex relationships and interactions (Elith et al., 2008). The algorithms modelled occurrence records (presence / absence) against biologically meaningful climatic predictors for marine forest species, while avoiding overfitting (i.e., complex fit of random noise) through monotonic responses (Hofner et al., 2011) and optimized parameterization procedures (Assis, Araújo, et al., 2017; Elith et al., 2008).

Climatic predictors for present-day conditions (climatology of 2000-2017), the warmer mid-Holocene (MH; ca. 6,000 years ago) and the Last Glacial Maximum (LGM; ca. 21,000 years ago) were downloaded from Bio-ORACLE (Assis, Tyberghein, et al., 2017; see data availability section); namely, nutrients (as nitrate and phosphate), salinity and ocean temperatures (maximum and minimum). These data considered the weighting of different Atmospheric-Ocean General Circulation Models (AOGCM; Assis, Tyberghein, et al., 2017) as well as the potential -120 m sea level change during the LGM (Assis et al., 2016, 2018; Peltier, 2004). Prior to modelling, Pearson's correlation coefficient was inferred between all pairs of predictors. Georeferenced presence records for the whole species distribution were compiled from a fine-tuned dataset of marine forests (Assis et al., 2020), while pseudo-absences were generated randomly to better calibrate models and isolate highly contributive

variables (Cerasoli et al., 2017). To account for sampling bias and restrict modelling to the actual extent of the species domain, pseudo-absences were chosen from a kernel probability surface produced with the presence records and a spatial grid with the same resolution as the climate data (Assis, Araújo, et al., 2017). To reduce the potential effect of spatial autocorrelation, the correlation of climatic predictors within the range of presence records was determined as a function of increasing marine distances using Mantel tests under 1×10^4 permutations (Boavida et al., 2016). The minimum non-correlated distance identified was used to trim records and remove overlapping surplus information.

Over-fitting and generalization were controlled by tuning BRT and AdaBoost hyperparameters (Assis, Araújo, et al., 2017; Fragkopoulou et al., 2021; Martins et al., 2021 for details) and by forcing monotonicity constrained responses (positive for salinity, nutrients and minimum temperature, and negative for maximum temperature; Hofner et al., 2011). A 10-fold cross-validation framework using independent latitudinal bands was implemented in this process (Assis, Araújo, et al., 2017). Models were produced with all combinations of BRT and AdaBoost parameters, fitting data interactively with one latitudinal band withheld at a time. The performance of each set of parameters was evaluated with the area under the curve of the receiver operating characteristic (AUC).

Final predictive models fitting occurrence records and predictor variables, and tuned with the optimal parameters (i.e., those retrieving higher average AUC values in cross-validation) were transferred to the climatologies of the LGM, MH and present to estimate the potential distribution of *L. pallida* through time. The predicted surfaces were reclassified to binomial surfaces representing presence and absences with a threshold maximizing sensitivity and specificity (true positive and negative rates, respectively; Allouche et al., 2006). Final performance scores were reported with AUC, sensitivity, and specificity. The ecological relevance of models was further assessed by determining the relative contribution of each climate predictor to the models (Elith et al., 2008), and by estimating physiological limits

points extracted from each climatic predictors, within the range of values found in the regions providing suitable conditions for the species, as inferred from the binomial predictive surfaces (Assis, Araújo, et al., 2017).

Biophysical modelling

Biophysical modelling was implemented following the approach of previous studies (Assis et al., 2021; Buonomo et al., 2016; Nicastro et al., 2019). This used data from the Hybrid Coordinate Ocean Model (HYCOM), a product providing daily current velocity fields at a resolution of 0.08° (approx. 6–9 km), and able to resolve complex eddies, meandering currents, fronts, and filaments (Chassignet et al., 2007), i.e., key mesoscale processes to simulate passively dispersing propagules (Assis et al., 2021).

The model comprised ~2250 km of coastlines, slightly exceeding the range of the species. A high-resolution polygon defining global landmasses (Haklay & Weber, 2008) limited the simulation. A rocky bottom cartography layer (Harris, 2012) was used to define source/sink sites along the coastline, 1 km apart, from which individual particles were released daily. Particles were allowed to passively drift for up to 30 days until they eventually reached the shore or were lost offshore. This period was considered extreme for long-lived rafts, in line with previous estimates for brown algae, including the closely related species *L. ochroleuca* (Assis et al., 2018; Monteiro et al., 2016). The geographic position of individual particles was determined hourly with bilinear interpolation over the velocity fields. Particle trajectories were aggregated as pairwise matrices representing the probability of connectivity between source/sink sites, by dividing the number of events a particle released from site *i* reached site *j*, by the total amount of particles released from site *i*. The potential inter-annual variability in ocean flow was assessed by running simulations individually for a period of 10 years (2008 to 2017), and by producing an averaged asymmetrical connectivity matrix.

The connectivity between the sites sampled for genetics was inferred by considering stepping-stone estimates of probability of connectivity (Assis et al., 2021; Buonomo et al., 2016). For this approach, graph theory was implemented, with nodes defined by site locations and edges by the probabilities of connectivity. The Floyd–Warshall’s algorithm, minimizing the sum of log-transformed probabilities, estimated the shortest connectivity paths between sites, from which probabilities were determined with a product function. As the actual dispersal period of *L. pallida* is unknown, an estimate was performed by comparing the marginal effect on Akaike information criterion (AIC) between linear models fitting probability of connectivity and genetic differentiation (Jost’s D), for the span of propagule durations simulated in the biophysical modelling (i.e., 1 to 30 days). The model retrieving the lowest AIC, i.e., best explaining differentiation, was used as a final estimate of the species’ potential dispersal period. Finally, two competing linear regression models were developed fitting genetic differentiation (Jost’s D) against (1) a null model of alongshore marine distances (i.e., isolation by distance model) and (2) a stepping-stone probability of connectivity tuned with the dispersal period previously inferred. The models were compared using adjusted R-square, Pearson’s correlation coefficient and Akaike information criteria (AIC).

Species distribution modelling, biophysical modelling and network analyses were performed using the R packages dismo, gbm, parallel, sdm SDMTools igraph, raster and vegan.

Results

Genetic diversity and structure

A total of 451 multi-locus genotypes were produced from the 20 sites sampled (n=442) plus the few drift algae (n=9) from 6 additional sites. Microsatellite polymorphism within the 14-loci dataset varied from 7 to 49 alleles per locus, with a mean of 16.64 alleles per locus. These data showed consistent evidence of null alleles in three loci (Ld158, Lo454-18 and Lo4-13; Table S2) and selection in three loci (Ld158, Lo454-24, Lo4-13; Table S3). To account for the potential effect of null alleles and selection in our results, an additional analysis of structure was performed without the potentially affected loci (i.e., Ld158, Lo454-24, Lo454-18 and Lo4-13). Because this did not change the main results (Fig. S1; Fig. 1), we did not exclude these loci from the analyses.

Within sites, standardized allelic richness (A), endemism (PA) and gene diversity (HE) were very variable (Table 1), with A showing a general increasing trend with latitude, with one exception for the southernmost site. In particular, the region comprising the sites from Hondeklip Bay to Jacobs Bay (South Africa; sites 17-22) exhibited the highest intra-population diversity levels, with A up to 7.76 ± 0.15 (Hondeklip, site 17), PA up to 5.75 ± 1.10 (Jacobs Bay, site 22) and HE up to 0.70 ± 0.01 (Doring Bay, site 18). Diversity was much lower at lower latitudes (central and northern Namibia), where A ranged between 2.9 and 3.96 ± 0.09 , whereas no PA were observed in 2 out of 5 populations (max. PA 0.43 ± 0.60 in Rocky Point, site 6). The lowest HEs were also found there (Mile 4 and Rocky Point, sites 9 and 6; Table 1).

Table 1. Genetic diversity of *Laminaria pallida* at each site based on 14 microsatellite loci. Code (#), region, site name, coordinates (Latitude and Longitude in decimal degrees), sample type (drift versus attached population), number of individuals (n), allelic richness (A), number of private alleles (PA) and Nei's gene diversity (expected heterozygosity; He). Diversity indices were estimated after standardizing the sample size to 20 individuals per population, where higher.

#	Region	Name	Lat	Lon	Type	n	A	PA	He
1	Namibia North	Bosluis Bay	-17.369	11.757	Drift	2	1.79		0.54
2	Namibia North	Portuguese Lorry	-17.559	11.735	Drift	2	2.07		0.54
3	Namibia North	Shipwreck	-19.140	12.592	Drift	1	1.36		0.19
4	Namibia North	False Cape Fria	-18.485	12.025	Drift	1	1.79		0.33
5	Namibia North	Angra Fria	-18.273	11.958	Drift	1	1.36		0.36
6	Namibia North	Rocky Point	-18.994	12.475	Attached	24	3.83±0.10	0.43±0.60	0.49±0.01
7	Namibia North	Moewe Bay	-19.369	12.705	Attached	24	3.96±0.09	0.15±0.36	0.50±0.01
8	Namibia North	Students Bay	-20.133	13.126	Drift	2	1.86		
9	Namibia North	Mile 4	-22.606	14.515	Attached	23	3.52±0.09		0.48±0.01
10	Namibia North	Henties Bay	-22.122	14.278	Attached	29	3.85±0.12	0.01±0.04	0.51±0.01
11	Namibia North	Swakopmund	-22.672	14.522	Attached	11	2.90		0.49
12	Namibia South	Sylvia Hill	-25.146	14.846	Attached	22	6.44±0.09	2.43±0.83	0.64±0.01
13	Namibia South	Spencer Bay	-25.709	14.847	Attached	24	6.09±0.11	1.28±0.74	0.64
14	Namibia South	Lüderitz	-26.646	15.149	Attached	24	6.22±0.15	2.30±0.59	0.59±0.01
15	South Africa North	Port Nolloth	-29.255	16.866	Attached	29	7.42±0.22	5.04±1.26	0.65±0.01
16	South Africa North	Kleinsee	-29.673	17.044	Attached	24	7.43±0.15	0.34±0.56	0.66±0.02
17	South Africa North	Hondeklip Bay	-30.315	17.27	Attached	24	7.76±0.15	3.01±1.02	0.66±0.01
18	South Africa North	Doring Bay 1	-31.814	18.233	Attached	20	7.21±0.10	3.22±0.44	0.70±0.01
19	South Africa North	Doring Bay 2	-31.814	18.233	Attached	24	7.35±0.16	2.21±0.84	0.67±0.01
20	South Africa Cape	Paternoster	-32.805	17.884	Attached	22	6.56±0.11	3.42±0.88	0.65
21	South Africa Cape	Jacobs Bay 1	-32.967	17.883	Attached	23	6.77±0.18	1.03±0.53	0.67
22	South Africa Cape	Jacobs Bay 2	-32.967	17.883	Attached	24	7.50±0.15	5.75±1.10	0.68
23	South Africa Cape	Mouille Point	-33.898	18.409	Attached	19	4.79±0.30	0.80	0.55±0.01
24	South Africa Cape	Oudekraal	-33.987	18.348	Attached	24	6.53±0.16	2.66±0.95	0.55±0.01
25	South Africa Cape	Kommetjie	-34.142	18.321	Attached	26	6.91±0.20	5.90±1.33	0.60±0.01
26	South Africa Cape	Stanford's Cove	-34.566	19.352	Attached	2	1.93		0.48

The ΔK criterion divided *L. pallida* into 2 main genetic clusters, with a narrow intermediate region of admixture (Fig. 1; Fig. S2): (1) the Namibia North cluster (northern group), including the sites from Bosluis Bay to Swakopmund (sites 1-11) and (2) the Namibia South - South Africa cluster (southern group), including the sites from Lüderitz (14, Namibia South) to

Stanford's Cove (site 26). The contact zone can be considered a third cluster (3), the Namibia overlap, a region of admixture including Sylvia Hill and Spencer Bay (sites 12-13). The southern group was further subdivided into smaller (K=3) subclusters although with weaker support (Fig. S2), but still showing stable compositions and a clear geographic signal (Fig. 1). Subclustering included the sites from Luderitz (site 14) to Doring Baai (site 19), and Paternoster (close to Cape Columbine) to Stanford's Cove (sites 20-26).

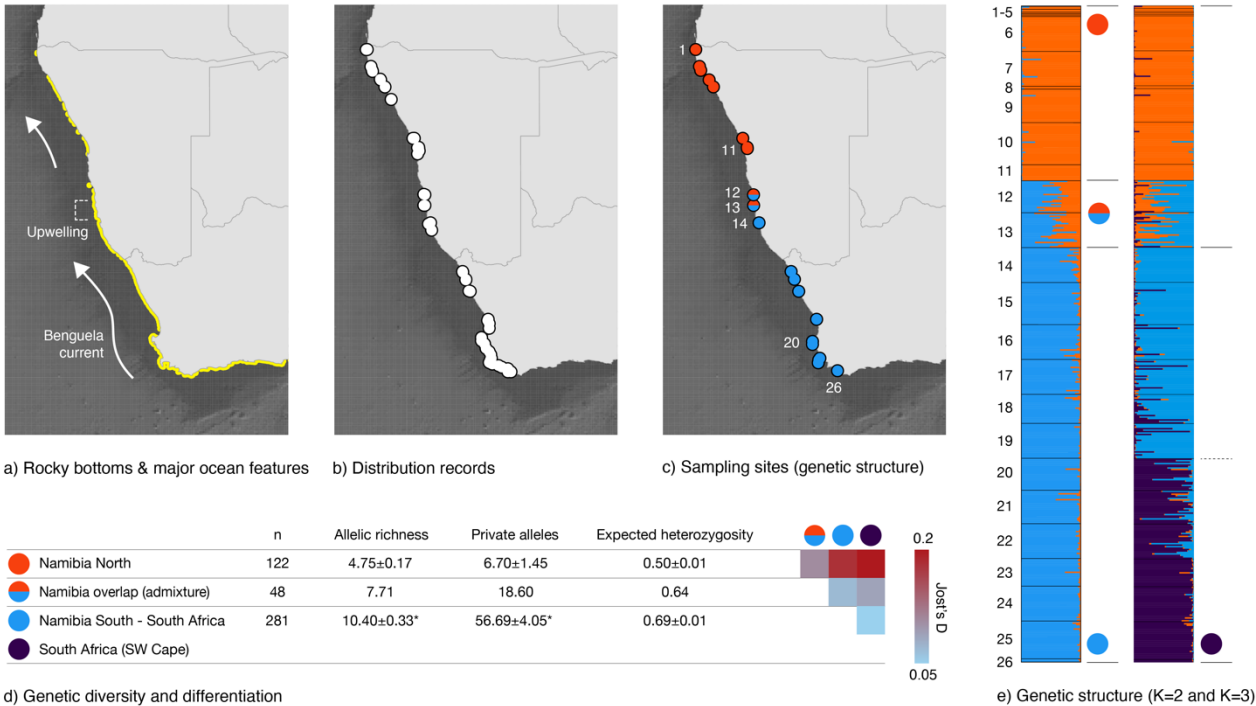
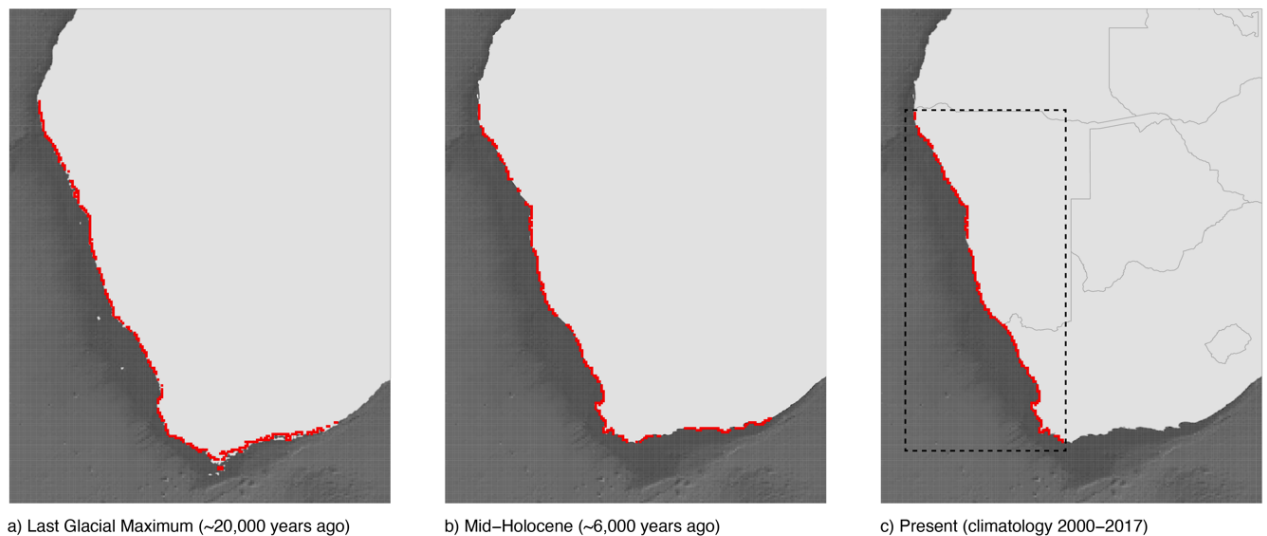


Figure 1. (panel a) Presence of rocky bottoms along the coastline (yellow) and major oceanographic patterns (Benguela current direction and the relative location of Lüderitz upwelling cell; Kämpf & Chapman, 2016), (panel b) records of *L. pallida* occurrence used in SDM and (panel c) sampling locations coloured according to the best supported number of genetic groups (K=2). (Panel d) Genetic diversity per cluster (K=2) as allelic richness, number of private alleles and Nei's gene diversity (expected heterozygosity), standardized for an equal-sized sample of 48 individuals (n). Pairwise genetic differentiation (as Jost's D) between genetic clusters. (Panel e) Genetic structure shown as individual assignments to genetic clusters (K=2 and K=3). Site names and coordinates are listed in Table 1.

The analysis of molecular variance (AMOVA) based on Jost's D showed significant differentiation levels within and between genetic clusters (Table S4). Differentiation levels were higher between the Namibia North and both southern sub-clusters (Jost's D > 0.15; Fig. 1) and lower between the admixture region (Namibia overlap) and both southern sub-clusters (Jost's D: 0.07 and 0.08; Fig. 1), as well as between both southern sub-clusters (Jost's D: 0.06; Fig. 1). Genetic diversity per cluster was significantly higher in Namibia South - South Africa cluster. This displayed more than two-fold allelic richness and nine-fold more private alleles when compared to the Namibia North cluster, and three-fold more private alleles when compared to the admixture region (Namibia overlap). Nei's gene diversity also followed a pattern of higher values in the southern cluster (Fig. 1).

Species distribution modelling



	AUC (Cross-validation)	AUC (Final)	Sensitivity (Final)	Specificity (Final)	True Skill Statistic
Boosted Regression Trees	0.95±0.05	0.97	0.97	0.93	0.90
Adaptive Boosting	0.96±0.04	0.96	0.97	0.91	0.88
Ensemble of algorithms	-	0.98	1	0.91	0.91

d) Species distribution modelling performance

Figure 2. Predicted distribution of *L. pallida* for (panel a) the Last Glacial Maximum, (b) the Mid-Holocene and (panel c) the present. Dashed polygon depicts the refugial region providing suitable conditions in the 3 time periods. (panel d) Performance of species

distribution modelling assessed with cross-validation and the final models predicting for present-day conditions.

Distribution models fitting the occurrence records (Fig. S3) and meaningful predictors showed high predictive performance, both when tested with independent data (cross-validation) and with the final prediction developed for present-day conditions (AUCs > 0.95; Sensitivity > 0.97; Specificity > 0.91; Fig. 2). The ensemble of algorithms accurately predicted the distribution of *L. pallida* (AUC: 0.98, Sensitivity = 1; Fig. 2). The most important predictors explaining the distribution of *L. pallida* (considering the region and resolution where the models were fitted) were maximum and minimum temperatures, as well as nutrients (relative contributions > 5%). Salinity had no contribution to the models (Fig. S4). These inferences are supported by the low correlation found between the pairs of predictors (Fig. S5); only temperatures (minimum and maximum) showed stronger correlation (Pearson's correlation > 0.85; Fig. S5), yet the forcing of opposite monotonic trends in the algorithms removed potential confounding effects about their relative contribution (Martins et al., 2021). The models predicted suitable habitats in regions with thermal conditions between 4.45°C (extreme temperature captured at Tristan da Cunha Island, where the species occurs; Fig. S2) and 21.89°C, and nutrient conditions of phosphate > 0.13 mmol.m³ and nitrate > 0.52 mmol.m³. A maximum limit of nutrients was not found along the species distribution.

The models revealed that past distributions could have been broader than today (Fig. 2). The equatorial distributional range of *L. pallida* could exceed the current border between Angola and Namibia (LGM ~200km displacement, compared to the present) and the eastward range could have been as far as East London in South Africa (LGM and MH ~750km displacement). The inferred refugial region providing suitable habitats across time included the complete current distributional limits of the species (Fig. 2).

Biophysical modelling

The biophysical model using HYCOM data over the ten-year period released a total of 1,293,162 particles. Particles drifting for the maximum 30-day period connected coastal sites at distances of 82.95 ± 64.53 km, on average, with a maximum connectivity distance of 526.50 km (Fig. S6). However, 95% of the connectivity events occurred over distances less than 215 km (Fig. S6).

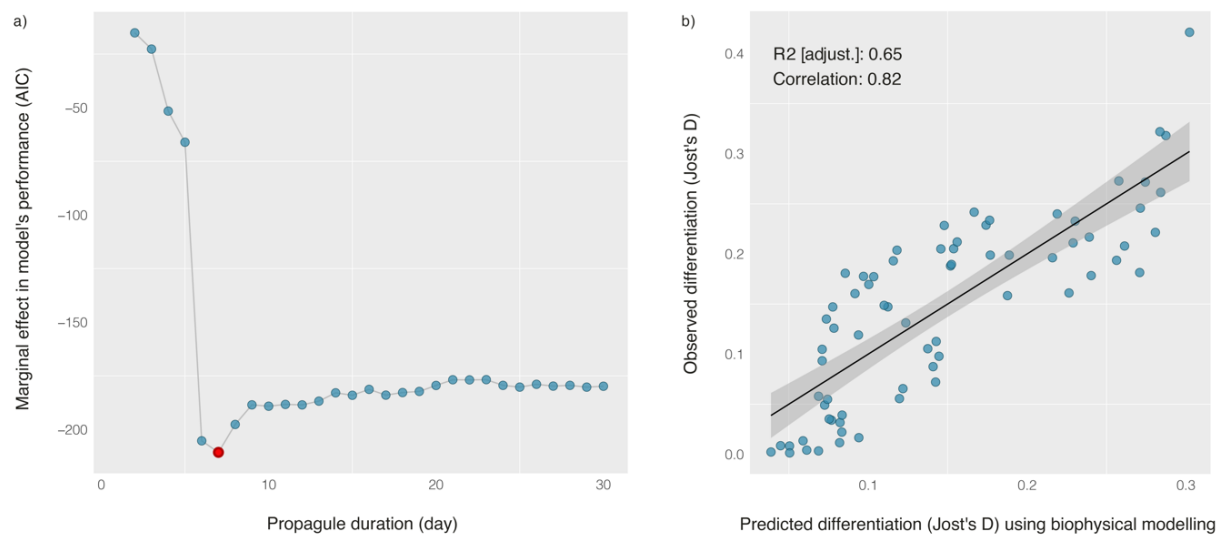


Figure 3. (panel a) Estimation of the potential dispersal period of *Laminaria pallida*. The red dot depicts the most likely dispersal period of the species (minimum AIC at day = 7). (panel b) Linear regression model fitting observed and predicted genetic differentiation (Jost's D) using probability of connectivity constrained to the optimal 7-day propagule duration.

The analysis comparing the marginal effect on AIC between models fitting probability of connectivity and population genetic differentiation identified a 7-day propagule duration for the species (Fig. 3). The connectivity estimates using this period outperformed the null model considering marine distances between paired populations (Fig. 3 vs. Fig. S7), i.e., habitat connectivity driven by ocean transport explained better the variability found in genetic data (adjusted R^2 : 0.63; Correlation: 0.81; Fig. 3).

430 Discussion

431 By combining empirical genetic data with theoretical modelling, this study demonstrates that
432 along the coastlines of southwestern Africa, intraspecific biodiversity can be highly structured
433 by habitat connectivity driven by oceanographic transport and barriers. In particular, two
434 main genetic clusters were identified, with their break matching a well-known dispersal
435 barrier to marine connectivity (Gunawickrama et al., 2020; Henriques et al., 2012, 2014, 2016;
436 Schulze et al., 2020), i.e., the strong upwelling front centred off Lüderitz. For kelp, an
437 additional constraint to stepping-stone dispersal is the discontinuity of rocky substrate along
438 this coastline. Contrarily to what was hypothesized, the impact of past range shifts might
439 have not been a major driver of the species' genetic structure (Nielsen et al., 2021). The SDM
440 estimated the past distribution of *L. pallida* even broader than today, with none of the present
441 populations potentially affected by extinctions and recolonization processes. No major
442 vicariant events, associated with past sea level changes and coastline displacements, were
443 further predicted. However, genetic diversity patterns are typical of those expected from a
444 lower latitude region that underwent major bottlenecks, as the two well-defined genetic
445 clusters differed strikingly in diversity, with much richer and unique levels in the southern
446 cluster (Namibia South - South Africa), compared to the northern cluster of Namibia North.
447 Limiting habitat conditions along the northern distribution, potentially eroding genetic
448 diversity levels, are hypothesized as the drivers explaining the observed patterns. Although
449 results indicate long-term climate suitability, they are also compatible with the hypothesis of
450 occasional short term heat waves causing local mass mortality events. Other factors,
451 occurring or even intensified in historical times, such as reduced availability of rocky reefs,
452 dust storms decreasing light availability, sand burial and sand scour (Engledow & Bolton,
453 1994), all likely to impact population sizes, are also compatible with our genetic results. The
454 importance and specific contexts of such events (e.g., in terms of location, timing and
455 intensity) is difficult to hindcast, but genetic diversity asymmetries suggest they have

impacted more intensely the northern range. Above all, genetic data reveal two distinct genetic clusters kept genetically isolated by the prevailing oceanographic patterns, giving them high conservation value in the face of future changes.

Long-term range stability across past climate changes

The distribution models retrieved good accuracy scores, as expected when fitting machine learning algorithms with compressive occurrence data and biologically meaningful predictors (Assis, Araújo, et al., 2017; M. R. Martins et al., 2021), and the main drivers shaping the distribution of *L. pallida* are corroborated by empirical studies. In particular, the inferred thermal range (between ca. 5 to 22°C) and nutrient conditions (phosphate > 0.1 and nitrate > 1 mmol.m³) providing suitable habitats match physiological experiments for this species (Martins et al., 2019) and the sister species *L. ochroleuca* (Assis et al., 2018). Transferring the algorithms to past climatologies (MH and LGM) revealed that the distribution of the species might have been broader than today; ~200 km northward during the LGM and ~750 km eastward during both LGM and MH. The northward range shifts likely resulted from the stronger upwelling conditions hypothesized during the LGM for the Benguela region (Romero et al., 2003), while the eastward shifts could have resulted from the weakening of the warmer Agulhas current during both LGM and MH periods (Hutson, 1980; Thackeray, 2016). These historical events might have reduced thermal stress conditions in both warm range edges, allowing range expansions and broadening distribution areas. The recent eastward range expansion of the kelp *Ecklonia maxima* (South Africa), beyond its historical range limit, possibly in response to recent cooling, illustrates well these responses (Bolton et al., 2012).

The inferred past range shifts of *L. pallida* contrasts with those reported for numerous kelp species in the North Atlantic, and the Southeast and Northeast Pacific. The current distribution of the species along ca. 2000 km of coastline was predicted to fit entirely within

a refugium providing long-term suitability from the LGM to the present. This is a unique case amongst kelps (inc. Laminariales and Tilopteridales; de Bettignies et al., 2021) for which multiple low latitude refugia were identified and corroborated both with SDM and genetic information (Assis et al., 2016, 2018; Fraser et al., 2009; Neiva et al., 2018; Song et al., 2021). Coastline displacements associated with sea level changes could have changed coastal geomorphology and type of substrata, potentially isolating populations of *L. pallida* (Phair et al., 2019; Toms et al., 2014). This was not predicted in our study, but the lack of data describing the past distribution of rocky reefs in the area precludes more accurate estimates. Hence, the models should be interpreted as estimates of fundamental niche conditions, and not fully realized niches. Additional sources of SDM uncertainty that should be acknowledge are related to the algorithms and climatologies used. The ensemble of BRT and AdaBoost, and weighting of different sources of climate data (distinct AOGCMs; Assis, Tyberghein, et al., 2017) allowed the partial assessment of uncertainty (Araújo & New, 2007). Accordingly, the climate data used in SDM mirrored the broadscale patterns of quality-controlled / independent data (Fig. S8). Yet, such independent data is limited to temperature for present-day and LGM conditions. If past conditions in southwestern Africa differed significantly from the patterns described in the data, SDM predictions overestimated actual distributions and therefore potential refugial areas.

Ocean currents driving genetic structure of *Laminaria pallida*

Our results recovered two well-defined genetic clusters with a region of admixture. These clusters display significant differentiation, suggesting the effect of isolation and drift. Each also contain many private alleles, indicating long-term persistence accumulating mutations that built up endemic diversity. This is in part corroborated by the distribution models predicting stable populations, or at least long-term suitable conditions. But despite such

temporal stability, the origin and persistence of the sharp genetic discontinuity must have been shaped by restricted gene flow across both regions, in insufficient levels to counteract genetic differentiation. Our results suggest that long-term oceanographic effects might have played a major role.

Biophysical modelling integrating the cartography of rocky substrate largely explained the observed patterns of genetic differentiation, and further suggested the possibility of dispersal by ocean currents up to 7 days. Considering the short spore longevity of kelps (Reed et al., 1992), a lower dispersal period was expected. However, *Laminaria* can be transported as viable floating fragments (Clarkin et al., 2012), which can be even found entangled in rafts of other algae (Susini et al., 2007). This is a well evidenced mechanism of marine dispersal (Clarkin et al., 2012) that might produce rare long-distance connectivity events (Batista et al., 2018), if the rafting fragments contain reproductive structures that release spores after dispersal to suitable areas. The genetic structure of *L. pallida* and other kelp species (Assis et al., 2016, 2018; Neiva et al., 2018) suggest that these events are rare, a premise corroborated by the biophysical modelling (Fig. S6), showing a skewed relationship between probability of connectivity and dispersal distances. The genetic composition of drifting algae, assigned to the adjacent “North Namibia” genetic group, is in line with these predictions.

Within the study region, the main mesoscale oceanographic processes revealed in the biophysical modelling to coincide with the species’ genetic structure are the strong upwelling conditions centred around the Lüderitz region, which coincides with the main barrier identified in the genetic data, and the prevalent patterns of the Benguela Current, promoting asymmetrical northward flow (Kämpf & Chapman, 2016; Stenevik et al., 2008). While the powerful offshore advection produced along the upwelling cell can generate a barrier to alongshore oceanographic transport, the flow of the Benguela current might homogenize within-cluster genetic structure, a pattern clearly observed in our data, particularly when considering the second level of structure ($K=3$). Previous studies also suggest that the

532 Lüderitz upwelling cell constitutes an ancient barrier to gene flow (potentially establishment
533 2 million years ago; Henriques et al., 2014) that promotes genetic differentiation for numerous
534 species (Gunawickrama et al., 2020; Henriques et al., 2012, 2014, 2016; Reid et al., 2016;
535 Schulze et al., 2020). Indeed, the bioregionalization proposed by (Spalding et al., 2007),
536 separating the Benguela realm into the Namib and Namaqua ecoregions, falls precisely in
537 the region where the main genetic barrier was observed. This strengthens our results, and
538 further supports the role of the Lüderitz upwelling cell in structuring the distribution of
539 biodiversity in southwestern Africa. The discontinuity of rocky shore habitats, also considered
540 in the biophysical modelling, could also play a role in isolation, yet less localized, affecting a
541 broader Namibian coastline. A second level of structure comprising an additional cluster
542 (Southwest Cape) was also identified, but with low statistical support and shallow genetic
543 differentiation. Nonetheless, the genetic barrier identified aligns with a finer scale
544 bioregionalization dividing the Namaqua region from the Southwestern Cape region (Griffiths
545 et al., 2010).

546 Our results also showed significantly higher and unique genetic diversity along the southern
547 range of *L. pallida*, in Namibia South and South Africa cluster, when compared to the distinct
548 genetic cluster of Namibia North. This is the opposite pattern of that reported for the isopod
549 *Tylos granulatus* along the same stretch of coastline (Mbongwa et al., 2019). As for other
550 *Laminaria* species, long-term persistence of large populations in the southern range might
551 have been crucial to accumulate and preserve genetic diversity (Assis et al., 2018). The lower
552 diversity observed along Namibia North can be explained by three exclusive hypotheses. The
553 first is extinction-recolonization of eroded Namibian habitats post-LGM, that could have
554 produced founder effects and bottlenecks along the colonization front (Assis et al., 2016;
555 Jenkins et al., 2018; Song et al., 2021). However, this finds no support from either distribution
556 modelling, nor the high genetic differentiation found between clusters, with unique alleles
557 also in the northern cluster. The second hypothesis, better supported by genetic evidence,

558 involves demographic effects related to small populations under limiting niche conditions
559 (Nicastro et al., 2013). The centre of the species distribution (circa Lüderitz) experiences
560 maximum monthly temperatures of ca. 15°C, while the northern populations experience
561 temperatures close to the 22°C tolerance limit of the species (as inferred from the models
562 and empirical evidence). Most importantly, heat wave events (Arafeh-Dalmau et al., 2020)
563 and periodic disruptions of the upwelling system (Hutchings et al., 2009) might impact
564 marginal populations due to temporarily reduced availability of cold, nutrient-rich waters.
565 Because no other Laminariales or Fucales (Engledow & Bolton, 1994) exist in northern
566 Namibia region, the potentially lower population sizes are unlikely to result from inter-specific
567 competition. Yet, intensive herbivory may play a role in controlling population sizes at such
568 lower latitudes (Steneck et al., 2017). The third hypothesis has to do with the limitation of
569 rocky shore area through time, along a very sandy coast in Namibia, as well as extinction-
570 recolonization dynamics due to rock burial/exposure. Such effects are likely on the northern
571 Namibian shores and might have taken place at varying degrees, more or less temporary
572 depending on sea-level variation (Peltier, 2004), sand burial of rocky substrate, sand scour
573 by storms, dust storms limiting light and covering rocks, all very limiting factors to persistence
574 of the essential microscopic stages of the kelp life-cycle, the gametophytic generation.

575 Overall, the present study demonstrates how one of the most globally important upwelling
576 systems can favour long-term population persistence, as well as structure oceanographic
577 conditions that create and maintain genetically distinct diversity across distributional ranges.
578 These particular conditions render *Laminaria pallida* a unique case among kelps, for which
579 the entire present distribution range was, according to the models, favourable since the LGM
580 to the present, supporting persisting populations at both range edges, which interestingly are
581 both warmer edges. Additionally, the oceanographic barrier posed by the upwelling might
582 have shaped the main genetic discontinuities of the species, which further coincided with
583 well-known biogeographic subdivisions. Considering the recent and projected intensification

of these conditions (Sydeman et al., 2014), it is likely that the observed genetic traits of *Laminaria pallida*, as well as those of species with similar niche requirements and distributions, will persist for the years to come (Lourenço et al., 2016), again contrasting with what has been observed and anticipated for numerous kelp forest species elsewhere (Arafah-Dalmau et al., 2020; Assis, Araújo, et al., 2017). Despite the general stability trend, the northernmost populations, with already reduced diversity levels, are prone to climate change impacts (Potts et al., 2014) and associated biodiversity losses, from the genetic to the ecosystem level. The distinct genetic diversity inferred between regions, coupled with the sharp isolation of phylogroups highlight their high conservation value in the face of future changes, particularly given the multiple ecological, social, and economic services provided by kelp forests (Blamey & Bolton, 2018) (Blamey & Bolton, 2018). As recently proposed for the region and elsewhere (Mertens et al., 2018; Nepper-davidsen et al., 2021), specific management and conservation actions might be required for divergent genetic lineages, as distinct drivers influence their levels of genetic diversity. The insights provided here are a significant step forward in the understanding of patterns and processes influencing marine biodiversity in southwestern Africa, and we hypothesize that they might be generalizable for other species with limited dispersal potential, which have been particularly overlooked in the region.

Acknowledgements

The CCMAR team received support from FCT - Foundation for Science and Technology (Portugal) through UIDB/04326/2020, SFRH/BSAB/150485/2019, the transitional norm - DL57/2016/CP1361/CT0035 and DL57/2016/CP1361/CT0010 and projects PTDC/MAR-EST/6053/2014 and PTDC/BIA-CBI/6515/2020, and from a Pew Marine Fellowship. Namibian sampling expeditions were funded by the Benguela Current Convention (BCC) through the project “Improving Ocean Governance in the Benguela Large Marine Ecosystem (BCLME III Project)” and with a generous financial contribution from the Global Environment Facility (GEF) and United Nations Development Programme (UNDP). JJB was funded by National Research Foundation fund number 111719.

Data availability statement

All data described in the Material and Methods section are openly available in Figshare at: <https://doi.org/10.6084/m9.figshare.17075177>

Biosketch

Jorge Assis is an assistant researcher at CCMAR. His research focuses on the biodiversity impacts of climate-induced range shifts at global scales.

João Neiva is an assistant researcher at CCMAR. His research focuses on the patterns and drivers of marine diversification and spatial genetic diversity and structure across seascapes, with particular emphasis on the role of past and ongoing climatic shifts, dispersal traits and hybridization.

630 **References**

- 631 Alberto, F., Raimondi, P. T., Reed, D. C., Watson, J. R., Siegel, D. A., Mitarai, S., Coelho,
632 N., & Serrão, E. A. (2011). Isolation by oceanographic distance explains genetic
633 structure for *Macrocystis pyrifera* in the Santa Barbara Channel. *Molecular Ecology*,
634 20(12), 2543–2554. <https://doi.org/10.1111/j.1365-294X.2011.05117.x>
- 635 Allouche, O., Tsoar, A., & Kadmon, R. (2006). Assessing the accuracy of species
636 distribution models: Prevalence, kappa and the true skill statistic (TSS). *Journal of*
637 *Applied Ecology*, 43(6), 1223–1232. <https://doi.org/10.1111/j.1365-2664.2006.01214.x>
- 638 Anderson, R. J., Bolton, J. J., Smit, A. J., & da Silva Neto, D. (2012). The Seaweeds of
639 Angola: The Transition Between Tropical and Temperate Marine Floras on the West
640 Coast of Southern Africa. *African Journal of Marine Science*, 34(1).
641 <https://doi.org/10.2989/1814232X.2012.673267>
- 642 Arafeh-Dalmau, N., Schoeman, D. S., Montaña-Moctezuma, G., Micheli, F., Rogers-
643 Bennett, L., Olguin-Jacobson, C., & Possingham, H. P. (2020). Marine heat waves
644 threaten kelp forests. *Science*, 367(6478), 635.
645 <https://doi.org/10.1126/science.aba5244>
- 646 Araújo, M. B., & New, M. (2007). Ensemble forecasting of species distributions. *Trends in*
647 *Ecology and Evolution*, 22(1), 42–47. <https://doi.org/10.1016/j.tree.2006.09.010>
- 648 Assis, J., Araújo, M. B., & Serrão, E. A. (2017). Projected climate changes threaten ancient
649 refugia of kelp forests in the North Atlantic. *Global Change Biology*, 24(1), 1365–2486.
650 <https://doi.org/10.1111/gcb.13818>
- 651 Assis, J., Coelho, N. C., Lamy, T., Valero, M., Alberto, F., & Serrão, E. A. (2016). Deep reefs
652 are climatic refugia for genetic diversity of marine forests. *Journal of Biogeography*,
653 43(4), 833–844. <https://doi.org/10.1111/jbi.12677>

654 Assis, J., Fragkopoulou, E., Frade, D., Neiva, J., Oliveira, A., Abecasis, D., Faugeron, S.,
 655 Serrão, E. A., Frade, D., Neiva, J., Oliveira, A., Abecasis, D., Faugeron, S., & Serrão, E.
 656 A. (2020). A fine-tuned global distribution dataset of marine forests. *Scientific Data*,
 657 7(1), 1–9. <https://doi.org/10.1038/s41597-020-0459-x>

658 Assis, J., Fragkopoulou, E., Serrão, E. A., Horta e Costa, B. arbara, Gandra, M., & Abecasis,
 659 D. (2021). Weak biodiversity connectivity in the European network of no-take marine
 660 protected areas. *Science of the Total Environment*, 773, 1–24.
 661 <https://doi.org/10.1016/j.scitotenv.2021.145664>

662 Assis, J., Serrão, E. A., C. Coelho, N., Tempera, F., Valero, M., & Alberto, F. (2018). Past
 663 climate changes and strong oceanographic barriers structured low - latitude genetic
 664 relics for the golden kelp *Laminaria ochroleuca*. *Journal of Biogeography*, 45(45),
 665 2326–2336. <https://doi.org/10.1111/jbi.13425>

666 Assis, J., Tyberghein, L., Bosch, S., Verbruggen, H., Serrão, E. A., & De Clerck, O. (2017).
 667 Bio-ORACLE v2.0: Extending marine data layers for bioclimatic modelling. *Global*
 668 *Ecology and Biogeography*, 27(3), 277–284. <https://doi.org/10.1111/geb.12693>

669 Batista, M. B., Sanches, P. F., Simionatto, P., Id, P., Cesar, T., Silveira, L., Velez-rubio, G.
 670 M., Scarabino, F., Camacho, O., Schmitz, C., Martinez, A., Ortega, L., Fabiano, G.,
 671 Rothman, M. D., Liu, G., Ojeda, J., Assis, J., Serrão, E. A., & Santos, R. (2018). Kelps '
 672 Long-Distance Dispersal: Role of Ecological / Oceanographic Processes and
 673 Implications to Marine Forest Conservation. *Diversity*.
 674 <https://doi.org/10.3390/d10010011>

675 Billot, C., Rousvoal, S., Estoup, A., Epplen, J. T., Saumitou-Laprade, P., Valero, M., &
 676 Kloareg, B. (1998). Isolation and characterization of microsatellite markers in the
 677 nuclear genome of the brown alga *Laminaria digitata* (Phaeophyceae). *Molecular*
 678 *Ecology*, 7(12), 1778–1780. <https://doi.org/10.1046/j.1365-294x.1998.00516.x>

679 Blamey, L. K., & Bolton, J. J. (2018). The economic value of South African kelp forests and
680 temperate reefs: Past, present and future. *Journal of Marine Systems*, 188(June), 172–
681 181. <https://doi.org/10.1016/j.jmarsys.2017.06.003>

682 Boavida, J., Assis, J., Silva, I., & Serrão, E. A. (2016). Overlooked habitat of a vulnerable
683 gorgonian revealed in the Mediterranean and Eastern Atlantic by ecological niche
684 modelling. *Scientific Reports*, 6(1), 36460. <https://doi.org/10.1038/srep36460>

685 Bolton, J. J., Anderson, R. J., Smit, A. J., & Rothman, M. D. (2012). South African kelp
686 moving eastwards: the discovery of *Ecklonia maxima* (Osbeck) Papenfuss at De Hoop
687 Nature Reserve on the south coast of South Africa. *African Journal of Marine Science*,
688 34(1), 147–151. <https://doi.org/10.2989/1814232X.2012.675125>

689 Bolton, J. J., & Stegenga, H. (2002). Seaweed species diversity in South Africa. *South*
690 *African Journal of Marine Science*, 24. <https://doi.org/10.2989/025776102784528402>

691 Buonomo, R., Assis, J., Fernandes, F., Engelen, A. H., Airoidi, L., & Serrão, E. A. (2016).
692 Habitat continuity and stepping-stone oceanographic explain population genetic
693 connectivity of the brown alga *Cystoseira amentacea*. *Molecular Ecology*.
694 <https://doi.org/http://dx.doi.org/10.5061/dryad.dk563>

695 Cerasoli, F., Iannella, M., D'Alessandro, P., & Biondi, M. (2017). Comparing pseudo-
696 absences generation techniques in Boosted Regression Trees models for conservation
697 purposes: A case study on amphibians in a protected area. *PLoS ONE*, 12(11), 1–23.
698 <https://doi.org/10.1371/journal.pone.0187589>

699 Chassignet, E. P., Hurlburt, H. E., Smedstad, O. M., Halliwell, G. R., Hogan, P. J., Wallcraft,
700 A. J., Baraille, R., & Bleck, R. (2007). The HYCOM (HYbrid Coordinate Ocean Model)
701 data assimilative system. *Journal of Marine Systems*, 65, 60–83.
702 <https://doi.org/10.1016/j.jmarsys.2005.09.016>

703 Clarkin, E., Maggs, C. A., Allcock, A. L., & Johnson, M. P. (2012). Environment, not
 704 characteristics of individual algal rafts, affects composition of rafting invertebrate
 705 assemblages in Irish coastal waters. *Marine Ecology Progress Series*, 470, 31–40.
 706 <https://doi.org/10.3354/meps09979>

707 Coelho, N. C., Serrão, E. A., & Alberto, F. (2014). Characterization of fifteen microsatellite
 708 markers for the kelp *Laminaria ochroleuca* and cross species amplification within the
 709 genus. *Conservation Genetics Resources*, 6(4), 949–950.
 710 <https://doi.org/10.1007/s12686-014-0249-x>

711 de Bettignies, T., Hébert, C., Assis, J., Bartsch, I., Bekkby, T., Christie, H., Dahl, K., Derrien-
 712 Courtel, S., Edwards, H., Filbee-Dexter, K., Franco, J., Gillham, K., Harrauld, M.,
 713 Hennicke, J., Hernández, S., Le Gall, L., Martinez, B., Mieszkowska, N., Moore, P., ...
 714 La Rivière, M. (2021). *Case report for kelp forest habitat* (OSPAR 787/2021 (ed.)).

715 Elith, J., Leathwick, J. R., & Hastie, T. (2008). A working guide to boosted regression trees.
 716 *Journal of Animal Ecology*, 77(4), 802–813. [https://doi.org/10.1111/j.1365-](https://doi.org/10.1111/j.1365-2656.2008.01390.x)
 717 [2656.2008.01390.x](https://doi.org/10.1111/j.1365-2656.2008.01390.x)

718 Engledow, H. R., & Bolton, J. J. (1994). Seaweed alpha-diversity within the lower eulittoral
 719 zone in namibia - the effects of wave action, sand inundation, mussels and limpets.
 720 *Botanica Marina*, 37(3), 267–276. <https://doi.org/10.1515/botm.1994.37.3.267>

721 Evanno, G., Regnaut, S., & Goudet, J. (2005). Detecting the number of clusters of
 722 individuals using the software STRUCTURE: A simulation study. *Molecular Ecology*,
 723 14(8), 2611–2620. <https://doi.org/10.1111/j.1365-294X.2005.02553.x>

724 Evans, B. S., Sweijd, N. A., Bowie, R. C. K., Cook, P. A., & Elliott, N. G. (2004). Population
 725 genetic structure of the perlemoen *Haliotis midae* in South Africa: Evidence of range
 726 expansion and founder events. *Marine Ecology Progress Series*, 270(May 2014), 163–

727 172. <https://doi.org/10.3354/meps270163>

728 Fragkopoulou, E., Serrão, E. A., Horta, P. A., Koerich, G., & Assis, J. (2021). Bottom
729 Trawling Threatens Future Climate Refugia of Rhodoliths Globally. *Frontiers in Marine*
730 *Science*, 7, 1–11. <https://doi.org/10.3389/fmars.2020.594537>

731 Fraser, C. I., Nikula, R., Spencer, H. G., & Waters, J. M. (2009). Kelp genes reveal effects of
732 subantarctic sea ice during the Last Glacial Maximum. *Proceedings of the National*
733 *Academy of Sciences of the United States of America*, 106(9), 3249–3253.
734 <https://doi.org/10.1073/pnas.0810635106>

735 Griffiths, C. L., Robinson, T. B., Lange, L., & Mead, A. (2010). Marine biodiversity in south
736 africa: An evaluation of current states of knowledge. In *PLoS ONE* (Vol. 5, Issue 8).
737 <https://doi.org/10.1371/journal.pone.0012008>

738 Gunawickrama, K. B. S., Delaval, A., Johansen, T., van der Plas, A. K., & Salvanes, A. G. V.
739 (2020). Genetic structure of *Sufflogobius bibarbatus* in the Benguela upwelling
740 ecosystem using microsatellite markers. *Journal of Applied Ichthyology*, 36(2), 168–
741 182. <https://doi.org/10.1111/jai.14002>

742 Haklay, M., & Weber, P. (2008). OpenStreet map: User-generated street maps. *IEEE*
743 *Pervasive Computing*, 7(4), 12–18. <https://doi.org/10.1109/MPRV.2008.80>

744 Harris, L. R. (2012). *BCLME shoreline mapping project 2011: A contract report to*
745 *Conservation Services for the Benguela Current Commission Spatial Biodiversity*
746 *Assessment*.

747 Henriques, R., Potts, W. M., Santos, C. V., Sauer, W. H. H., & Shaw, P. W. (2014).
748 Population connectivity and phylogeography of a coastal fish, *Atractoscion aequidens*
749 (Sciaenidae), across the Benguela Current region: Evidence of an ancient vicariant
750 event. *PLoS ONE*, 9(2). <https://doi.org/10.1371/journal.pone.0087907>

751 Henriques, R., Potts, W. M., Sauer, W. H. H., & Shaw, P. W. (2012). Evidence of deep
 752 genetic divergence between populations of an important recreational fishery species,
 753 *Lichia amia* L. 1758, around southern Africa. *African Journal of Marine Science*, 34(4).
 754 <https://doi.org/10.2989/1814232X.2012.749809>

755 Henriques, R., von der Heyden, S., Lipinski, M. R., du Toit, N., Kainge, P., Bloomer, P., &
 756 Matthee, C. A. (2016). Spatio-temporal genetic structure and the effects of long-term
 757 fishing in two partially sympatric offshore demersal fishes. *Molecular Ecology*, 25(23).
 758 <https://doi.org/10.1111/mec.13890>

759 Hofner, B., Müller, J., & Hothorn, T. (2011). Monotonicity-constrained species distribution
 760 models. *Ecology*. <https://doi.org/10.1890/10-2276.1>

761 Hutchings, L., van der Lingen, C. D., Shannon, L. J., Crawford, R. J. M., Verheye, H. M. S.,
 762 Bartholomae, C. H., van der Plas, A. K., Louw, D., Kreiner, A., Ostrowski, M., Fidel, Q.,
 763 Barlow, R. G., Lamont, T., Coetzee, J., Shillington, F., Veitch, J., Currie, J. C., &
 764 Monteiro, P. M. S. (2009). The Benguela Current: An ecosystem of four components.
 765 *Progress in Oceanography*, 83(1–4). <https://doi.org/10.1016/j.pocean.2009.07.046>

766 Hutson, W. H. (1980). The Agulhas current during the Late Pleistocene: Analysis of modern
 767 faunal analogs. *Science*, 207(4426), 64–66.
 768 <https://doi.org/10.1126/science.207.4426.64>

769 Jenkins, T. L., Castilho, R., & Stevens, J. R. (2018). Meta-analysis of northeast Atlantic
 770 marine taxa shows contrasting phylogeographic patterns following post-LGM
 771 expansions. *PeerJ*, 2018(9). <https://doi.org/10.7717/peerj.5684>

772 Kämpf, J., & Chapman, P. (2016). *The Benguela Current Upwelling System BT - Upwelling*
 773 *Systems of the World: A Scientific Journey to the Most Productive Marine Ecosystems*
 774 (J. Kämpf & P. Chapman (eds.); pp. 251–314). Springer International Publishing.

775 https://doi.org/10.1007/978-3-319-42524-5_7

776 Keenan, K., McGinnity, P., Cross, T. F., Crozier, W. W., & Prodöhl, P. A. (2013). diveRsity:
 777 An R package for the estimation and exploration of population genetics parameters
 778 and their associated errors. *Methods Ecol Evol*, 4(8), 782–788.
 779 <https://doi.org/10.1111/2041-210X.12067>

780 Lourenço, C. R., Nicastro, K. R., McQuaid, C. D., Chefaoui, R. M., Assis, J., Taleb, M. Z., &
 781 Zardi, G. I. (2017). Evidence for rangewide panmixia despite multiple barriers to
 782 dispersal in a marine mussel. *Scientific Reports*, 1–16. [https://doi.org/10.1038/s41598-](https://doi.org/10.1038/s41598-017-10753-9)
 783 017-10753-9

784 Lourenço, C. R., Zardi, G. I., McQuaid, C. D., Serrão, E. A., Pearson, G. A., Jacinto, R., &
 785 Nicastro, K. R. (2016). Upwelling areas as climate change refugia for the distribution
 786 and genetic diversity of a marine macroalga. *Journal of Biogeography*, 43(8), 1595–
 787 1607. <https://doi.org/10.1111/jbi.12744>

788 Maggs, C. A., Castilho, R., Foltz, D., Henzler, C., Jolly, M. T., Kelly, J., Olsen, J., Perez, K.
 789 E., Stam, W., Väinölä, R., Viard, F., & Wares, J. (2008). Evaluating signatures of glacial
 790 refugia for north atlantic benthic marine taxa. *Ecology*, 89(11), S108–S122.
 791 <https://doi.org/10.1890/08-0257.1>

792 Martins, M. R., Assis, J., & Abecasis, D. (2021). *Biologically meaningful distribution models*
 793 *highlight the benefits of the Paris Agreement for demersal fishing targets in the North*
 794 *Atlantic Ocean. April*, 1–14. <https://doi.org/10.1111/geb.13327>

795 Martins, N., Pearson, G., Gouveia, L., Tavares, A. I., Serrão, E. A., & Bartsch, I. (2019).
 796 Hybrid vigour for thermal tolerance in hybrids between the allopatric kelps *Laminaria*
 797 *digitata* and *L. pallida* (Laminariales, Phaeophyceae) with contrasting thermal affinities.
 798 *European Journal of Phycology*, 54(4).

799 <https://doi.org/10.1080/09670262.2019.1613571>

800 Mbongwa, Hui, C., Pulfrich, A., & S, von der H. (2019). Every beach an island - deep
801 population divergence and possible loss of genetic diversity in *Tylos granulatus*, a
802 sandy shore isopod. *Marine Ecology Progress Series*, 614, 111–123.

803 Meirmans, P. G., & Van Tienderen, P. H. (2004). GENOTYPE and GENODIVE: Two
804 programs for the analysis of genetic diversity of asexual organisms. *Molecular Ecology*
805 *Notes*, 4(4), 792–794. <https://doi.org/10.1111/j.1471-8286.2004.00770.x>

806 Mertens, L. E. A., Treml, E. A., & von der Heyden, S. (2018). Genetic and biophysical
807 models help define marine conservation focus areas. *Frontiers in Marine Science*,
808 5(AUG). <https://doi.org/10.3389/fmars.2018.00268>

809 Monteiro, C. A., Paulino, C., Jacinto, R., Serrão, E. A., & Pearson, G. A. (2016). Temporal
810 windows of reproductive opportunity reinforce species barriers in a marine broadcast
811 spawning assemblage. *Scientific Reports*, 6, 29198.

812 Neiva, J., Paulino, C., Nielsen, M. M., Krause-Jensen, D., Saunders, G. W., Assis, J.,
813 Bárbara, I., Tamigneaux, É., Gouveia, L., Aires, T., Marbà, N., Bruhn, A., Pearson, G.
814 A., & Serrão, E. A. (2018). Glacial vicariance drives incipient speciation in the amphi-
815 boreal kelp *Saccharina latissima*. *Scientific Reports*, June 2017, 1–12.
816 <https://doi.org/10.1038/s41598-018-19620-7>

817 Nepper-Davidsen, J., Magnusson, M., Glasson, C. R. K., Ross, P. M., & Lawton, R. J.
818 (2021). Implications of Genetic Structure for Aquaculture and Cultivar Translocation of
819 the Kelp *Ecklonia radiata* in Northern New Zealand. *Frontiers in Marine Science*, 8,
820 1744. <https://doi.org/10.3389/fmars.2021.749154>

821 Nepper-davidsen, J., Magnusson, M., Glasson, C. R. K., Ross, P. M., Lawton, R. J.,
822 Portnoy, D. S., & Nepper-davidsen, J. (2021). *Implications of Genetic Structure for*

823 *Aquaculture and Cultivar Translocation of the Kelp Ecklonia radiata in Northern New*
824 *Zealand*. 8(November), 1–11. <https://doi.org/10.3389/fmars.2021.749154>

825 Nicastro, K. R., Assis, J., Serrão, E. A., Pearson, G. A., Valero, M., Jacinto, R., & Zardi, G. I.
826 (2019). Congruence between fine-scale genetic breaks and dispersal potential in an
827 estuarine seaweed across multiple transition zones. *ICES Journal of Marine Science*.
828 <https://doi.org/10.1093/icesjms/fsz179>

829 Nicastro, K. R., Zardi, G. I., Teixeira, S., Neiva, J., Serrao, E. A., Pearson, G. A., Serrão, E.
830 A., & Pearson, G. A. (2013). Shift happens: trailing edge contraction associated with
831 recent warming trends threatens a distinct genetic lineage in the marine macroalga
832 *Fucus vesiculosus*. *BMC Biology*, 11(1), 6. <https://doi.org/10.1186/1741-7007-11-6>

833 Nielsen, E. S., Beger, M., Henriques, R., & von der Heyden, S. (2021). Neither historical
834 climate nor contemporary range fully explain the extant patterns of molecular diversity
835 in marine species. *Journal of Biogeography*, 48(10). <https://doi.org/10.1111/jbi.14229>

836 Peltier, W. R. (2004). Global glacial isostasy and the surface of the ice-age earth: the ice-5g
837 (vm2) model and grace. In *Annual Review of Earth and Planetary Sciences* (Vol. 32, pp.
838 111–149). <https://doi.org/10.1146/annurev.earth.32.082503.144359>

839 Phair, N. L., Toonen, R. J., Knapp, I., & Von Der Heyden, S. (2019). Shared genomic outliers
840 across two divergent population clusters of a highly threatened seagrass. *PeerJ*,
841 2019(4). <https://doi.org/10.7717/peerj.6806>

842 Potts, W. M., Henriques, R., Santos, C. V., Munnik, K., Ansorge, I., Dufois, F., Booth, A. J.,
843 Kirchner, C., Sauer, W. H. H., & Shaw, P. W. (2014). Ocean warming, a rapid
844 distributional shift, and the hybridization of a coastal fish species. *Global Change*
845 *Biology*, 20(9). <https://doi.org/10.1111/gcb.12612>

846 Pritchard, J. K., Stephens, M., & Donnelly, P. (2000). Inference of population structure using

847 multilocus genotype data. *Genetics*, 155(2), 945–959. <https://doi.org/10.1111/j.1471->
848 8286.2007.01758.x

849 R Development Core Team. (2021). R: A Language and Environment for Statistical
850 Computing. In *R: A Language and Environment for Statistical Computing*. R
851 Foundation for Statistical Computing.

852 Reed, D. C., Amsler, C. D., & Ebeling, A. W. (1992). Dispersal in kelps: factors affecting
853 spore swimming and competency. *Ecology*, 73(73), 1577–1585.
854 <https://doi.org/10.2307/1940011>

855 Reid, K., Hoareau, T. B., Graves, J. E., Potts, W. M., Dos Santos, S. M. R., Klopper, A. W., &
856 Bloomer, P. (2016). Secondary contact and asymmetrical gene flow in a cosmopolitan
857 marine fish across the Benguela upwelling zone. *Heredity*, 117(5).
858 <https://doi.org/10.1038/hdy.2016.51>

859 Robinson, N. M., Nelson, W. A., Costello, M. J., Sutherland, J. E., & Lundquist, C. J. (2017).
860 A systematic review of marine-based Species Distribution Models (SDMs) with
861 recommendations for best practice. In *Frontiers in Marine Science* (Vol. 4, Issue DEC).
862 <https://doi.org/10.3389/fmars.2017.00421>

863 Romero, O., Mollenhauer, G., Schneider, R. R., & Wefer, G. (2003). Oscillations of the
864 siliceous imprint in the central Benguela Upwelling System from MIS 3 through to the
865 early Holocene: The influence of the Southern Ocean. *Journal of Quaternary Science*,
866 18(8), 733–743. <https://doi.org/10.1002/jqs.789>

867 Rothman, M. D., Bolton, J. J., Stekoll, M. S., Boothroyd, C. J., Kemp, F. A., & Anderson, R.
868 J. (2017). Geographical variation in morphology of the two dominant kelp species,
869 Ecklonia maxima and Laminaria pallida (Phaeophyceae, Laminariales), on the west
870 coast of Southern Africa. *Journal of Applied Phycology*, 29(5).

871 <https://doi.org/10.1007/s10811-017-1255-7>

872 Rothman, M. D., Mattio, L., Anderson, R., & Bolton, J. J. (2017). A phylogeographic
873 investigation of the kelp genus *Laminaria* (Laminariales, Phaeophyceae), with
874 emphasis on the South Atlantic Ocean. *Journal of Phycology*, March.
875 <https://doi.org/10.1111/jpy.12544>

876 Schulze, M. J., von der Heyden, S., Japp, D., Singh, L., Durholtz, D., Kapula, V. K., Ndjaula,
877 H. O. N., & Henriques, R. (2020). Supporting Fisheries Management With Genomic
878 Tools: A Case Study of Kingklip (*Genypterus capensis*) Off Southern Africa. *Frontiers in*
879 *Marine Science*, 7. <https://doi.org/10.3389/fmars.2020.557146>

880 Silva, G., Horne, J. B., & Castilho, R. (2014). Anchovies go north and west without losing
881 diversity: Post-glacial range expansions in a small pelagic fish. *Journal of*
882 *Biogeography*, 41, 1171–1182. <https://doi.org/10.1111/jbi.12275>

883 Song, X.-H., Assis, J., Zhang, J., Gao, X., Choi, H.-G., Duan, D.-L., Serrão, E. A., & Hu, Z.-
884 M. (2021). Climate-induced range shifts shaped the present and threaten the future
885 genetic variability of a marine brown alga in the Northwest Pacific. *Evolutionary*
886 *Applications*, n/a(n/a). <https://doi.org/https://doi.org/10.1111/eva.13247>

887 Spalding, M. D., Fox, H. E., Allen, G. R., Davidson, N., Finlayson, M. A. X., Halpern, B. S.,
888 Jorge, M. A., Lombana, A. L., Lourie, S., Martin, K. D., Molnar, J., Recchia, C., &
889 Robertson, J. (2007). Marine Ecoregions of the World: A Bioregionalization of Coastal
890 and Shelf Areas. *BioScience*, 57(7), 573–583. <https://doi.org/10.1641/B570707>

891 Steneck, R. S., Bellwood, D. R., & Hay, M. E. (2017). Herbivory in the marine realm. In
892 *Current Biology* (Vol. 27, Issue 11). <https://doi.org/10.1016/j.cub.2017.04.021>

893 Stenevik, E. K., Verheye, H. M., Lipinski, M. R., Ostrowski, M., & Strømme, T. (2008). Drift
894 routes of Cape hake eggs and larvae in the southern Benguela current system. *Journal*

895 *of Plankton Research*, 30(10), 1147–1156. <https://doi.org/10.1093/plankt/fbn068>

896 Susini, M.-L., Thibaut, T., Meinesz, A., & Forcioli, D. (2007). A preliminary study of genetic
897 diversity in *Cystoseira amentacea* (C. Agardh) Bory var. *stricta* Montagne (Fucales,
898 Phaeophyceae) using random amplified polymorphic DNA. *Phycologia*, 46(6), 605–611.
899 <https://doi.org/10.2216/06-100.1>

900 Sydeman, W. J., Garcia-Reyes, M., Schoeman, D. S., Rykaczewski, R. R., Thompson, S. A.,
901 Black, B. A., & Bograd, S. J. (2014). Climate change and wind intensification in coastal
902 upwelling ecosystems. *Science*, 345(6192), 77–80.
903 <https://doi.org/10.1126/science.1251635>

904 Teske, P. R., Golla, T. R., Sandoval-Castillo, J., Emami-Khoyi, A., Van Der Lingen, C. D.,
905 Von Der Heyden, S., Chiazari, B., Jansen Van Vuuren, B., & Beheregaray, L. B. (2018).
906 Mitochondrial DNA is unsuitable to test for isolation by distance. *Scientific Reports*,
907 8(1). <https://doi.org/10.1038/s41598-018-25138-9>

908 Teske, P. R., Heyden, S., McQuaid, C. D., Barker, N. P., Von der Heyden, S., McQuaid, C.
909 D., & Barker, N. P. (2011). A review of marine phylogeography in southern Africa. *S Afr*
910 *J Sci*, 107(5/6), 1–11. <https://doi.org/10.4102/sajs.v107i5/6.514>

911 Teske, P. R., Mcquaid, C. D., Froneman, P. W., & Barker, N. P. (2006). *Impacts of marine*
912 *biogeographic boundaries on phylogeographic patterns of three South African*
913 *estuarine crustaceans*. 314(Harrison 2002), 283–293.

914 Teske, P. R., Sandoval-Castillo, J., Golla, T. R., Emami-Khoyi, A., Tine, M., Von Der
915 Heyden, S., & Beheregaray, L. B. (2019). Thermal selection as a driver of marine
916 ecological speciation. *Proceedings of the Royal Society B: Biological Sciences*,
917 286(1896). <https://doi.org/10.1098/rspb.2018.2023>

918 Thackeray, J. F. (2016). Comparison of Holocene temperature data (Boomplaas Cave) and

919 oxygen isotope data (Cango Caves). In *South African Journal of Science* (Vol. 112,
920 Issues 5–6). <https://doi.org/10.17159/sajs.2016/a0156>

921 Toms, J. A., Compton, J. S., Smale, M., & Von Der Heyden, S. (2014). Variation in palaeo-
922 shorelines explains contemporary population genetic patterns of rocky shore species.
923 *Biology Letters*, 10(6), 12–15. <https://doi.org/10.1098/rsbl.2014.0330>

924 Toonen, R. J., & Hughes, S. (2001). Increased throughput for fragment analysis on an ABI
925 Prism 377 automated sequencer using a membrane comb and STRand software.
926 *BioTechniques*, 31, 1320–1324.

927 Van Oosterhout, C., Hutchinson, W. F., Wills, D. P. M., Shipley, P., Oosterhout, C.,
928 Hutchinson, W. F., Wills, D. P. M., & Shipley, P. (2004). MICRO-CHECKER: Software
929 for identifying and correcting genotyping errors in microsatellite data. *Molecular*
930 *Ecology Notes*, 4(3), 535–538. <https://doi.org/10.1111/j.1471-8286.2004.00684.x>

931 Von der Heyden, S., Gildenhuys, E., Bernardi, G., & Bowie, R. C. K. (2013). Fine-scale
932 biogeography: tidal elevation strongly affects population genetic structure and
933 demographic history in intertidal fishes. *Frontiers of Biogeography*, 5(1).
934 <https://doi.org/10.21425/f5fbg13391>

935 Whitlock, M. C. (2011). GST and D do not replace FST. *Molecular Ecology*, 20(6), 1083–
936 1091. <https://doi.org/10.1111/j.1365-294X.2010.04996.x>

937 Yeh, F. C., & Boyle, J. . (1997). POPGENE, the user-friendly shareware for population
938 genetic analysis. *Molecular Biology and Biotechnology*, 434.

939

940